Electroactive Methacrylate-Based Triblock Copolymer Elastomer for Actuator Application

Kie Yong Cho,[1,2] Seung Sang Hwang,[1,3] Ho Gyu Yoon,[2] Kyung-Youl Baek[1,3]

[1]Center for Materials Architecturing, Korea Institute of Science and Technology, Seoul 136-791, Korea
[2]Department of Material Science, Korea University, Seoul 136-701, Korea
[3]Nanomaterials Science and Engineering, University of Science and Technology, Daejeon 305-333, Korea
Correspondence to: K.-Y. Baek (E-mail: mailto:baek@kist.re.kr)

Received 10 July 2012; accepted 15 December 2012; published online 19 February 2013
DOI: 10.1002/pola.26563

ABSTRACT: A series of ABA triblock copolymers of methyl methacrylate (MMA) and dodecyl methacrylate (DMA) [poly (MMA-*b*-DMA-*b*-MMA)] (PMDM) were synthesized by Ru-based sequential living radical polymerization. For this, DMA was first polymerized from a difunctional initiator, ethane-1,2-diyl *bis* (2-chloro-2-phenylacetate) with combination of $RuCl_2(PPh_3)_3$ catalyst and nBu_3N additive in toluene at 80 °C. As the conversion of DMA reached over about 90%, MMA was directly added into the reaction solution to give PMDM with controlled molecular weight ($M_w/M_n \leq 1.2$). These triblock copolymers showed well-organized morphologies such as body centered cubic, hexagonal cylinder, and lamella structures both in bulk and in thin film by self-assembly phenomenon with different poly(methyl methacrylate) (PMMA) weight fractions. Obtained PMDMs with 20–40 wt % of the PMMA segments showed excellent electroactive actuation behaviors at relatively low voltages, which was much superior compared to conventional styrene-ethylene-butylene-styrene triblock copolymer systems due to its higher polarity derived from the methacrylate backbone and lower modulus. © 2013 Wiley Periodicals, Inc. J. Polym. Sci., Part A: Polym. Chem. **2013**, *51*, 1924–1932

KEYWORDS: atom transfer radical polymerization; block copolymers; elastomers; microstructure; stimuli-sensitive polymers

INTRODUCTION Electroactive polymers (EAPs) have gained much attention as promising candidates for next generation compact actuators, sensors, artificial muscles, and micro robotics, owing to large electromechanical deformation, high energy density, fast response time, and facile proccessability.[1–5] Among several EAP materials such as conductive,[6] ferroelectric,[7] and so forth, dielectric elastomers (DE) are especially interesting because of their large deformation with fast recovery, making them suitable for artificial muscle applications.[8]

Actuation with DE materials have been so far carried out with chemically crosslinked elastic rubbers such as acrylic and silicon polymers, with a recent report of styrene-ethylene-butylene-styrene (SEBS) triblock copolymer with mineral oil additives showing superior electromechanical performance at relatively low operating voltages.[4,8] This electromechanical performance was attributed to the self-assembled morphology of the block copolymer, which allowed for enhanced electrostatic Maxwell stress. Critical parameters of thickness strain (S_z) of DE are dielectric constant (k) and modulus (Y), described by the equation [$S_z = k\varepsilon_0(V/z)^2/Y$], where ε_0 is permittivity at free space, V is applied voltage, z is the thickness.[9] Thus, DE materials generally require higher dielectric constant and lower modulus for optimal actuation performance.

However, these previous systems utilizing SEBS triblock copolymers have had intrinsic limitations on high actuation performance, because its non-polar hydrocarbon chain possesses a relatively low dielectric constant ($k \fallingdotseq 2$) as well as the use of oil additives for softness (elasticity) which may flow out during operation. To overcome this, more polar and elastomeric block copolymers such as acrylate or methacrylate based block copolymers ($k \fallingdotseq 4$) without any oil additives are considered as interesting alternative materials.[10] Various kinds of well-defined acrylate or methacrylate based di- and triblock copolymers with hard-soft-hard structure, for example, triblock copolymers consisting of poly(methyl methacrylate) (PMMA) as a hard block segment in conjunction with poly(*n*-butyl acrylate), poly(dodecyl methacrylate) (PDMA), polyisobutylene, or polybutadiene as a soft block segment, were already reported using living polymerization techniques such as living anionic and radical polymerizations.[11–14] However, their elastomeric properties were relatively inferior compared to SEBS or styrene-isoprene-styrene (SIS) block copolymers, which was probably due to unclear long ranged ordered phase separations and weak

physical crosslinked hard PMMA domains. Fortunately for this actuation application, such large deformation was not necessary (thickness strain $< 71\%$),[8] the strains from the acrylate or methacrylate based triblock copolymer elastomers might be enough to cover deformation ranges. Furthermore, the actuation performance in this system would be enhanced by increased polarity (k) originated from the acrylate or methacrylate groups in comparison to the SEBS.

In this study, a series of well-defined hard-soft-hard methyl methacrylate (MMA)-dodecyl methacrylate (DMA)-MMA triblock copolymers (PMDMs) were synthesized by living radical polymerization, especially atom transfer radical polymerization (ATRP) to examine their actuation property without oil additive.[15,16] Syntheses of these triblock copolymers by ATRP have already been discussed using Cu-based catalytic system.[12] However, those by Ru-based system have yet to be examined, especially by *in situ* direct addition of the second monomer to the reaction solution of the precursor, which is a more convenient method because of no cumbersome isolation process of the precursor. Obtained PMDMs with different molecular weights and compositions were characterized their morphologies both in bulk and in thin film states. Actuation performances with those PMDM were then carried out at different electric fields and the relationship of the actuation with their microstructure changes was examined.

EXPERIMENTAL

Materials

All chemicals were purchased from Aldrich and used without purification process unless mentioned otherwise. Ethane-1,2-diyl *bis*(2-chloro-2-phenylacetate (EDBCPA) was prepared by a modified literature procedure (see below).[17] MMA (Aldrich, 99%), tributylamine (n-Bu_3N) (Aldrich, $\geq$98.5%) and toluene (Aldrich, 99.8%) was purified by vacuum distillation with calcium hydride before use. DMA (Aldrich, 96%) was purified by passing through an inhibitor remover column (Aldrich, AL-154) without pressure.

Synthesis of Ethane-1,2-diyl bis(2-chloro-2-phenylacetate) Difunctional Initiator

In a 300 mL round-bottom flask filled with nitrogen, 2-chloro-2-phenylacetyl chloride (7.5 g, 40 mmol) was added dropwise to a solution of ethylene glycol (0.993 g, 16 mmol) and anhydrous triethylamine (3.235 g, 32 mmol) in anhydrous THF (150 mL) at 0 °C. The solution was stirred at 0 °C for 10 min and then at 25 °C for an additional 10 h. The solution was then evaporated to remove THF and methylene chloride (200 mL) was added, and then poured into distilled water (200 mL). The organic solution was then separated and extracted with saturated sodium hydrogen carbonate three times, followed by deionized water three times. The organic layer was then collected and dried over sodium sulfate for overnight. After filtration and evaporation of the solution under vacuum, a yellowish crude product was obtained, which was further purified by chromatography on silica using ethyl acetate and hexane (1:4) as eluent (3.1 g, yield: 44.4%).

^{1}H NMR analysis: δ 4.28 ppm (m, 4H, CH_2), 5.27 ppm (d, 2H, CH), 7.33 ppm (m, 6H, H_{ar}), 7.43 ppm (m,4H, H_{ar}).

Polymerization PROCEDURE of MMA-DMA-MMA Triblock Copolymer

The polymerizations were carried out by the syringe technique under argon using baked flasks with three-way stopcocks. A typical procedure with DMA/EDBCPA/$RuCl_2(PPh_3)_3$/n-Bu_3N/MMA follows: In a 100 mL round-bottom flask was placed $RuCl_2(PPh_3)_3$ (0.1 mmol, 95.9 mg), toluene (10 mL), n-Bu_3N (0.4 mmol, 1 mL, 400 mM in toluene), DMA (20 mmol, 5.86 mL), and a solution of EDBCPA (0.1 mmol, 0.25 mL, 400 mM in toluene) was added sequentially in this order at 25 °C under argon. The reaction solution was then placed in a oil bath set at 80 °C. After the polymerization reached ca. 90% conversion for 24 h, MMA (50 mmol, 5.35 mL) was rapidly added to the unquenched solution. The reaction terminated by cooling down to −78 °C. The conversions at predetermined times were determined by integration ratio of ^{1}H NMR spectra of the polymer and the unreacted monomer, which was directly achieved from the reaction solution. The quenched reddish solution was then diluted with THF (10 mL) and then vigorously shaken with neutralized aluminum oxide. After filtering aluminum oxide, the solution was collected and solvents were removed by reduced pressure. The concentrated solution was dropped into methanol. Obtained white rubber-like solid was decanted and then dried at 25 °C for 48 h under vacuum.

Bulk Sample Preparation for Small Angle X-Ray Scattering

A solution of the PMDM (10 wt % in THF) was filtered by 0.45 μm syringe filter and then poured onto a Teflon petridish, which was slowly dried in atmosphere at 25 °C and further dried in the vacuum oven at 25 °C for overnight. After separating PMDM from the petridish, PMDM casted film was secured covering the pin-hole of the brass small angle X-ray scattering (SAXS) holder and subsequently annealed at 170 °C in the vacuum oven for 3 days. After the annealing process, the samples were slowly cooled to 25 °C.

Thin Film Sample Preparation for Atomic Force Microscope

Solutions of the PMDM ($\sim$2.5 wt % in toluene) were filtered by 0.2-μm syringe filter and spin coated on 2 $\times$ 2 cm^2 silicon wafer at 1500 rpm for 60 s. Silicon wafers were previously treated by piranha solution followed by rinsed using IPA, acetone, and distilled water in order to make a hydrophilic surface. Obtained thin film sample was dried at 25 °C overnight and annealed at 170 °C in the vacuum oven for 3 days. After the annealing process, the samples were slowly cooled to 25 °C.

Actuation Sample Preparation

A solution of the PMDM (10 wt % in THF) was filtered by 0.45 μm syringe filter and then poured onto a teflon petridish, which was slowly dried in atmosphere at 25 °C and further dried in the vacuum oven at 25 °C for overnight. After separating the PMDM films from the petridish, the films were pressed using 2 $\times$ 2 cm^2 molder at 170 °C. Obtained

PMDM sheets were further annealed at 170 °C in vacuum oven for 3 days, when conductive carbon grease was stenciled on both sides of the sheet as a compliant electrode.

Characterization

The number average molecular weight (M_n) and molecular weight distributions (M_w/M_n) of the samples were measured using a JASCO PU-2080 plus SEC system equipped with RI-2031 and a UV-2075 (254-nm detection wavelength) using THF as an eluent at 40 °C with 1 mL/min of the flow rate. The samples were separated through four columns: Shodex-GPC KF-802, KF-803, KF-804, and KF-805. PMMAs were used as calibration standards for SEC analysis. ^{1}H NMR spectra were taken in $CDCl_3$ at 25 °C on a 300 MHz Varian Unity INOVA. Thermal gravimetric analysis (TGA) was performed by TA instrument (TGA 2950) under nitrogen. Differential scanning calorimeter (DSC) was performed by TA instrument (TA Q20-142653) under nitrogen. Tapping mode atomic force microscope (AFM) measurement was performed by Multimode 8 with Nanoscope V controller (Veeco), which equipped with a E-type vertical engage scanner at RT. Synchrotron SAXS was performed at 4C1 SAXS beam line in Pohang Light Source. All conditions for 4C1 beam line followed literature procedure.[18] Dynamic mechanical analysis was performed by dynamic mechanical analyzer (DMA Q800, TA instruments) under nitrogen. Tensile modulus was determined using a universal test machine (H5KT, Tinius Olsen) with a cross header speed of 10 mm/min. Thickness strain (S_z) for actuation test was measured by incident laser beam which were exposed vertically to the sheet surface during a voltage applied. The sheet was located between two lasers, of which deviations generated by actuation were detected by photo-responsive sensor. The measurement system consists of a high voltage amplifier (Trek 10110B), a function generator (Agilent 33251A), a laser sensor set (Keyence LK-G80) and a sample holder.[19]

RESULTS AND DISCUSSION

A series of ABA triblock copolymers of MMA and DMA were synthesized by sequential living radical polymerization with $RuCl_2(PPh_3)_3$ catalyst and n-Bu_3N additive in toluene at 80 °C (Scheme 1).[17]

For this, ethane-1,2-diyl bis(2-chloro-2-phenylacetate) (EDBCPA) (**A**) was first synthesized and used as a difunctional alkyl halide initiator to polymerize with DMA (**B**), which gave PDMA as the first block segment precursor.

Figure 1 shows the number average molecular weight (M_n), polydispersity (M_w/M_n), and size exclusion chromatography scans (SEC, PMMA std.) of the obtained PDMA as the conversion increased. The polymerization proceeded smoothly with increase of the conversion to 90% (24 h) and the M_n corresponded well with the theoretical value. The polydispersity was relatively broad (PDI < 1.5) at early conversions ($\sim$50%) but it became narrow on the end of the polymerization (PDI $= 1.26$). As the conversion of DMA reached over 90%, MMA as a second monomer was directly added to the reaction solution. Added MMA was then polymerized from both chloride end groups of the PDMA chain to give hard-soft-hard MMA-DMA-MMA triblock copolymer (PMDM) (**C**). The molecular weight (M_n) of the PMDM linearly increased with increase of the conversion to 80% (37 h). SEC curves of the PMDMs also shifted to higher molecular weight fraction in comparison to the PDMA precursor with narrow polydispersity (PDI $= 1.21$) (Fig. 2). These results indicated that the Ru catalyzed living radical polymerization was particularly well suited for a one pot system to synthesize well-defined PMDMs.

Obtained PDMA precursor and PMDM were then analyzed by ^{1}H NMR spectroscopy (Fig. 3). The PDMA precursor obtained after 24 h ($M_n = 43{,}900$; PDI $= 1.26$) showed the characteristic peaks originating from the ester dodecyl protons (*e–f*), the α-methyl protons (*b*), and the methylene protons (*a*) of the main backbone [Fig. 3(A)]. However, it was difficult to figure out the peaks from the initiating moieties in the center of the PDMA and the ω-end moiety adjacent of the chlorine atom, which was probably due to relatively high molecular weight. The product obtained after the block copolymerization of MMA from the PDMA precursor ($M_n = 79{,}000$; PDI $= 1.21$) showed additional peaks from the ester methyl protons (*g*), the α-methyl protons (*b′*), and the methylene protons (*a′*) of the PMMA [Fig. 3(B)], which indicated that the PMDM was successfully synthesized as shown in Scheme 1. Weight fraction of this block copolymer was achieved by peak integration ratios of the ester methylene (*c*) and methyl (*g*) of the PDMA and the PMMA block

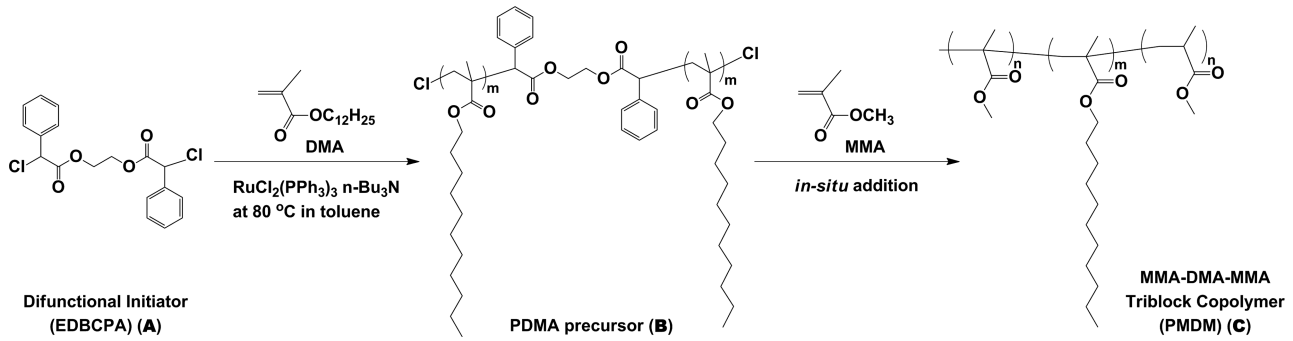

SCHEME 1 Synthesis of MMA-DMA-MMA triblock copolymer by sequential block copolymerization of DMA and MMA from difunctional initiator (EDBCPA) by Ru-catalyzed living radical polymerization.

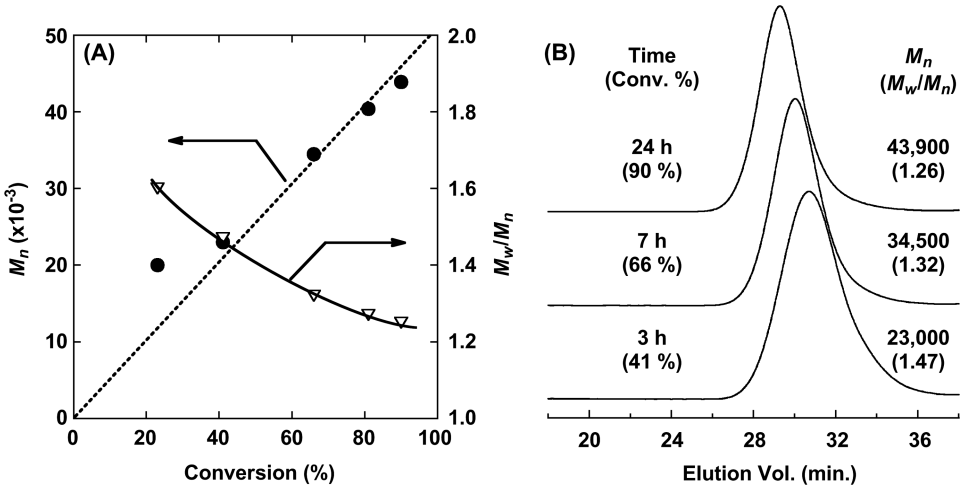

FIGURE 1 M_n and MWD curves of PDMA precursors obtained from EDBCPA/ $RuCl_2(PPh_3)_3$/*n*-Bu_3N (10/10/40 mM) in toluene at 80 °C: $[DMA]_0 = 2$ M.

segments, respectively. Table 1 shows series of the PDMAs and the PMDMs with different molecular weights (M_n) and weight fractions (15–46 wt %). Run 1–5 and 6–11 were the PMDMs from the PDMA precursors with lower molecular weighs (M_n = 43,900–53,500) and higher molecular weights (M_n = 70,300–74,600), respectively. The number averaged molecular weights ($M_{n,NMR}$) of the PMDMs calculated from ^{1}H NMR analyses were well corresponded with those ($M_{n,SEC}$) from SEC analyses, especially for the lower molecular weight series (run 1–5), while the higher molecular weight series (run 6–11) showed relatively higher $M_{n,NMR}$ than $M_{n,SEC}$, probably due to the significantly larger hydrodynamic volume changes in comparison to the smaller molecular weight series. Thus, the forthcoming number averaged molecular weight (M_n) for the PMDM was used as that based on ^{1}H NMR analysis.

Thermal property of the PMDM was characterized by thermogravimetric analysis (TGA) and differential scanning calorimetry (DSC). Figure 4(A) shows the TGA curve of the PMDM with 45 wt % of the PMMA (M_n = 88,900, run 4) at a heating rate of 10 °C/min under nitrogen. Decomposition started at 180 °C and complete decomposition was observed at 442 °C. These decomposition behaviors were in good agreement with those of the PDMA and PMMA homopolymers. Figure 4(B), a-c shows the DSC curve of the PDMA (M_n = 72,300), the PMMA (M_n = 16,300), and the PMDM with 30 wt % of the PMMA (M_n = 68,900, run 2). The temperature scan ranged from −80 to 170 °C at a heating rate of 10 °C/min under nitrogen. The glass transition temperatures (T_g) of PDMA and PMMA were observed at −49 and 119.5 °C, while those block segments of the PMDM appeared at −51.3 and 98.7 °C, respectively, where the T_g of the PMMA block segment was a little lower than that from the PMMA homopolymer, probably due to lower molecular weight of the PMMA block segment (M_n = 25,000/2) or contamination of DMA in the PMMA block segment during the block copolymerization of MMA. From these thermal analyses results,

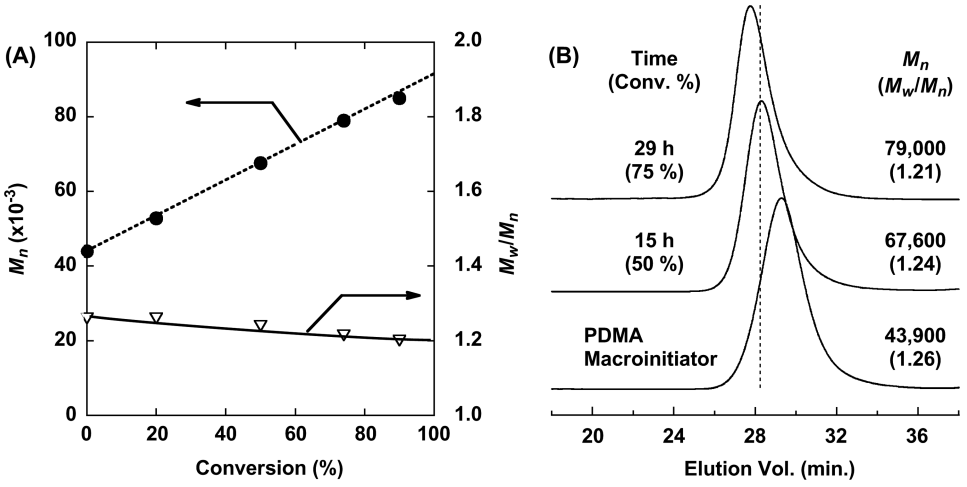

FIGURE 2 M_n and MWD curves of MMA-DMA-MMA triblock copolymers obtained by *in situ* addition of MMA when DMA conversion reached over 90%: $[MMA]_0 = 5$ M.

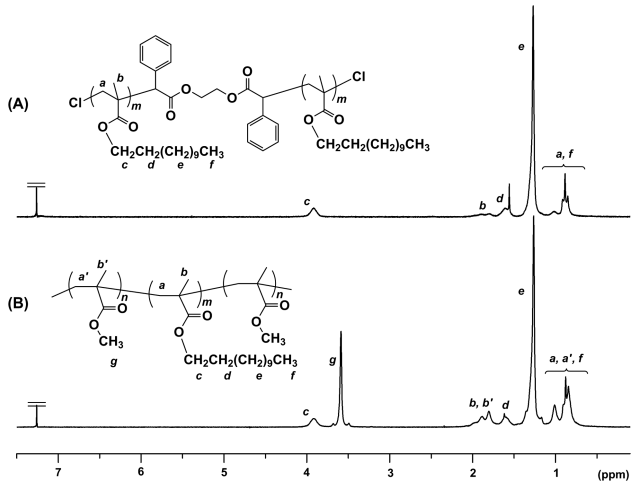

FIGURE 3 ^{1}H NMR spectra of (A) PDMA precursor and (B) MMA-DMA-MMA triblock copolymer at room temperature in $CDCl_3$.

optimized annealing conditions were ascertained to achieve ordered morphology of the PMDM.

Morphology of the PMDM triblock copolymers were then characterized both in bulk and in thin film states by SAXS and AFM, respectively, because a well-defined morphology of the triblock copolymer strongly affects actuation performance. Figure 5 shows the SAXS profiles of the PMDMs with different molecular weights and weight fractions, where Figure 5(A) consisted of the lower molecular weight series (run 1–4) and Figure 5(B) consisted of the higher molecular weight series (run 6–9) as shown in Table 1. All samples were thermally annealed at 170 °C for 3 days under vacuum. Both PMDM series showed long ranged ordered X-ray scattering profiles regardless of the PMMA weight fractions, which were more clearly observed in the higher molecular weight series because segregation of block copolymer was strongly affected by the parameter χN, where χ is Flory–Huggins interaction parameter and N is the degree of polymerization of the copolymer (molecular weight).[20,21] The domain sizes of these triblock copolymers ($d = 2\pi/q^*$) enlarged as the PMMA weight fractions increased, which ranged from 22 to 45 nm (Table 1). The PMDM with 15 wt % of the PMMA weight fraction showed typical body centered cubic (BCC) structured scattering patterns, $1q{:}\sqrt{2}q{:}\sqrt{3}q{:}\sqrt{4}q{:}\sqrt{5}q{:}\sqrt{6}q{:}\sqrt{7}q$ [Fig. 5(B-a)], however that with 18 wt % showed unclear periodic patterns [Fig. 5(A-a)], which was probably the phase transition between sphere and cylinder structures. The PMMA weight fractions ranged from 30 to 39 wt % also showed long ranged ordered multiple patterns, $1q{:}\sqrt{3}q{:}\sqrt{4}q{:}\sqrt{7}q{:}\sqrt{9}q{:}\sqrt{13}q$, indicating the formation of hexagonal packed cylinder structures (HEX) [Fig. 5(A,b-c, B, b-c)]. The PMDM with over 40 wt % of the PMMA showed clear lamella structures with typical ordering patterns of 1q:2q:3q:4q:5q [Fig. 5(A-d, B-d)].

Surface morphologies of the PMDMs were then characterized by AFM (Fig. 6). Thin film samples were prepared by spin coating process on silicon wafer followed by thermal annealing at 170 °C for 3 days under vacuum. The SAXS profile of the PMDM with 18 wt % of the PMMA showed unclear periodic scattering patterns [Fig. 5(A-a)], however its AFM image showed clear embossed patterns on the film surface [Fig. 6(A)]. The cylinder structured PMDMs as shown in Figure 5 (30–39 wt % of the PMMA) showed laterally laid domains of the PMMA on the silicon wafer, of which domain size increased as the molecular weight increased (Fig. 6, B and C for the lower molecular weight series and E–G for the higher molecular weight series).[22] In addition, the shapes of the lateral cylinder domains with the higher PMMA weight

TABLE 1 Various PDMA Precursors and MMA-DMA-MMA Triblock Copolymers with Different Molecular Weights and Weight Fractions

	PDMA Precursor		MMA-DMA-MMA Triblock Copolymer (PMDM)					
Run	$M_{n,SEC}$	M_w/M_n	$M_{n,SEC}$	M_W/M_N	$M_{n,NMR}$	PMMA (wt %)	Microstructure	d (nm)
1[a]	43,900	1.26	52,800	1.26	54,000	18	BCC/HEX	21.6
2[a]	43,900	1.26	67,600	1.24	68,900	30	HEX	24.5
3[a]	43,900	1.26	79,000	1.21	81,400	39	HEX	28.0
4[a]	43,900	1.26	85,000	1.20	88,900	45	LAM	28.7
5[b]	54,500	1.23	75,800	1.20	82,500	17	BCC	22.2
6[b]	71,700	1.22	88,700	1.21	91,700	15	BCC	27.8
7[c]	73,500	1.36	93,400	1.35	112,500	30	HEX	34.9
8[c]	73,500	1.36	114,000	1.30	146,600	38	HEX	38.5
9[c]	73,500	1.36	140,000	1.29	163,600	46	LAM	45.2
10[b]	70,300	1.21	86,000	1.19	101,300	26	HEX	25.8
11[a]	74,600	1.26	109,000	1.27	109,500	29	HEX	30.5

[a] [DMA]/[MMA]/[$RuCl_2(PPh_3)_3$]/[Bu_3N]/[EDBCPA] = 2 M/5 M/10 mM/40 mM/10 mM in toluene at 80 °C.
[b] [DMA]/[MMA]/[$RuCl_2(PPh_3)_3$]/[Bu_3N]/[EDBCPA] = 1.5 M/2.5 M/5 mM/20 mM/5 mM in toluene at 80 °C.
[c] [DMA]/[MMA]/[$RuCl_2(PPh_3)_3$]/[Bu_3N]/[EDBCPA] = 1.75 M/5 M/5 mM/20 mM/5 mM in toluene at 80 °C.

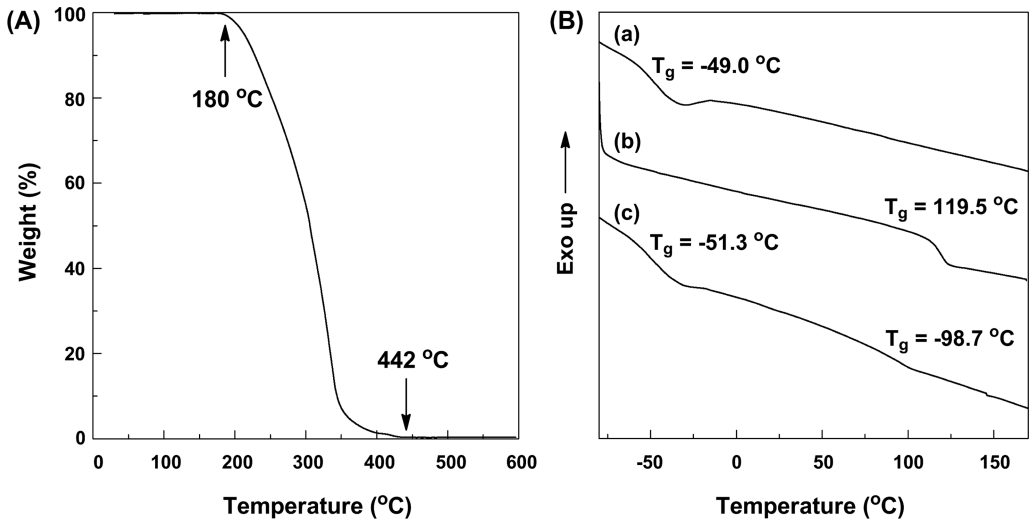

FIGURE 4 Thermal properties of MMA-DMA-MMA triblock copolymers: (A) TGA curves of PMDM (M_n = 85,000, PMMA = 45 wt %) and (B) DSC curves of (a) PDMA (M_n = 72,300), (b) PMMA (M_n = 16,000), (c) PMDM (M_n = 67,600, PMMA = 30 wt %). Heating and/or cooling rate = 10 °C/min under nitrogen.

fractions [Fig. 6(C, F–G)]were less extended than those with the lower PMMA weight fraction series [Fig. 6(B,E)]. The surface morphology of the low molecular weight PMDM with 45 wt % of the PMMA fraction was similar to those with the cylinder structured series in spite of the lamella structure as shown in Figure 5(A-d), which indicated that the lamella domains stood vertically to the surface [Fig. 6(D)]. However, the high molecular weight PMDM with similar weight fraction (46%) laid horizontally on the surface [Fig. 6(H)], which was probably due to the susceptibility of the smaller polymer chains to the surface between the silicon wafer and air in the lamella structures. From these results, we found that the PMMA and the PDMA of the triblock copolymers were not miscible to show efficient phase separations both in bulk and in film states, especially more periodic ordering microstructures in bulk states, which was important to show better actuation performance.

The elastomeric properties of these well-defined triblock copolymers were then characterized using dynamic mechanical analyzer (DMA), especially with 26 wt % (run 10) and 45 wt % (run 4) of the PMMA. The scanning range of temperature was from −80 to 140 °C with a heating rate of 4 °C/min. Figure 7(A) shows the temperature dependence of storage modulus (G') and tan δ. Both samples showed two characteristic G' losses at the points close to the glass transition temperatures of the PDMA and the PMMA as well as

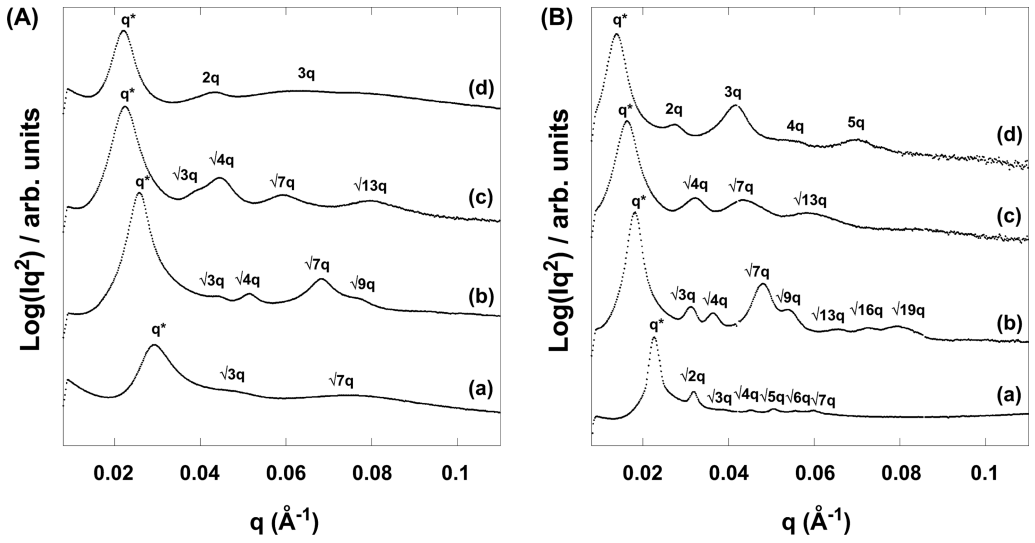

FIGURE 5 SAXS profiles of MMA-DMA-MMA triblock copolymers in bulk states: (A) low molecular weight series with (a) 18%, (b) 30%, (c) 39%, and (d) 45% of PMMA weight fractions (run 1–4); (B) high molecular weight series with (e) 15%, (f) 30%, (g) 38%, and (h) 46% of PMMA weight fractions (run 6–9). See Table 1.

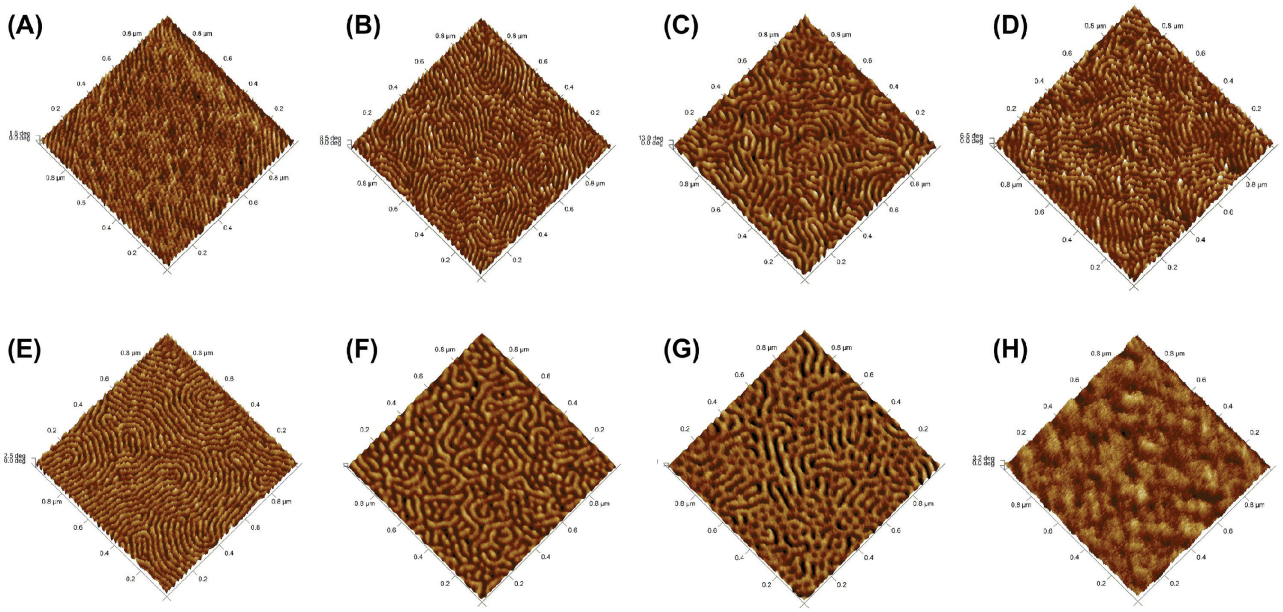

FIGURE 6 Tapping mode AFM images of MMA-DMA-MMA triblock copolymers in thin film states: (A-D) low molecular weight series with (A) 18%, (B) 30%, (C) 39%, and (D) 45% of PMMA weight fractions (run 1–4); (E–H) high molecular weight series with (E) 26%, (F) 30%, (G) 38%, and (H) 46% of PMMA weight fractions (run 7–10). See Table 1.

rubbery G' plateaus between them, indicating microphase separation of the soft PDMA and the hard PMMA domains, which is generally observed from conventional block copolymer elastomers.[23] The PMDM with the lower PMMA weight fraction (26%) showed more sharp losses of G' than that with the higher PMMA weight fraction (45%), which indicated that softer PMDM showed more elastomeric behavior. The glass transition temperatures obtained from tan δ were a little underestimated in comparison to those from DSC, especially the PMDM with the lower PMMA weight fraction, probably due to low frequency set in DMA measurement, of which phenomenon was also observed in the previous studies.[12] Tensile properties of the PMDMs with various PMMA weight fractions were examined by universal testing machine (UTM). The samples were prepared by hot press molding method at 170 °C for 10 min and expended with 10 mm/min with preload 1 g. Figure 7(B, a-c) shows tensile stress–strain curves of the PMDMs with 17 wt % (run 5), 29 wt % (run 10), and 45 wt % (run 4) of the PMMAs, respectively. Although the entire tensile properties of the PMDMs were inferior to conventional SEBS or SIS block copolymer elastomers, the relatively softer PMDMs with 17 and 29 wt % of the PMMAs, had modulus values of 0.14 and 0.53 MPa, respectively, showed classical elastic behaviors within 50%

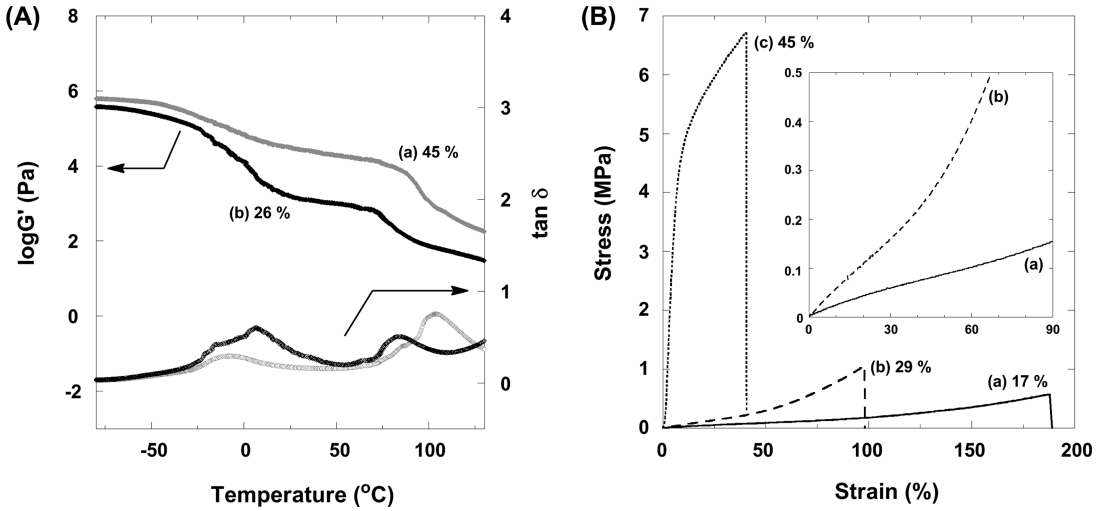

FIGURE 7 Elastic and tensile properties of MMA-DMA-MMA triblock copolymers: (A) DMA analyses for temperature dependence storage modulus (G') and tan δ with (a) 26% and (b) 45% of PMMA weight fractions (run 10 and 4) and (B) UTM analyses for stress–strain curves with (a) 17%, (b) 29%, and 45% of PMMA weight fractions (run 4–5 and run 11). See Table 1.

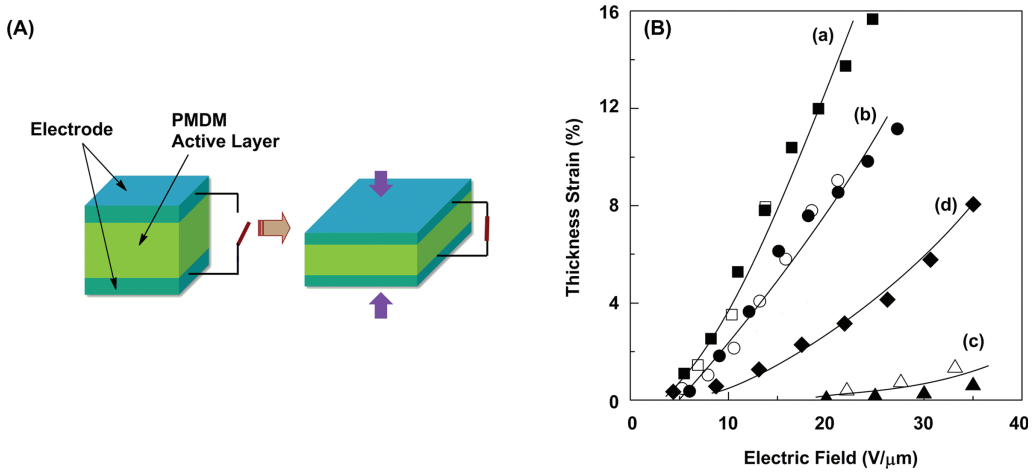

FIGURE 8 Actuation performances of MMA-DMA-MMA triblock copolymers: (A) illustration of actuation operation at voltage on/off and (B) thickness strain changes (S_z, %) with increasing electric field (V/μm). Open symbols for low molecular weights: (a) 30 wt %, (b) 39 wt %, and (c) 45% of PMMA weight factions (run 2–4) and closed symbols for high molecular weights: (a) 30%, (b) 38%, (c) 46% of PMMA weight factions (run 6–8). (d) Conventional SEBS system (M_n = 100,000, 30 wt % of the polystyrene) for comparison. See Table 1.

of the strain ranges [Fig. 7(B, inset)],[14] which were elongated to 98 and 200%, respectively. This strain range was sufficiently enough to perform for the actuation applications. However, the PMDM with the high PMMA weight fraction (45%) showed high modulus (87.9 MPa) and poor elongation at break point (40%). From these results, more soft and elastic PMDMs with the lower weight fractions of PMMAs were employed for forthcoming actuation tests.

Actuation tests with these triblock copolymers were conducted by measuring the change of the thickness strain by 2-laser system with external electric field source.[24] For this, thin sheet samples were prepared by hot press molding method at 170 °C, which were further thermally annealed at 170 °C for 3 days under vacuum, followed by stenciling with a conductive carbon grease compliant on both sides as an electrode [Fig. 8(A)]. Figure 8(B) showed thickness strain changes of the PMDMs with different weight fractions and molecular weights with increase in electric fields (operating voltage). As the PMMA weight fractions decreased, the softness of the PMDM increased, and the thickness strain changed to a larger degree. For example, the PMDMs with ca.45 wt % of the PMMA fractions showed merely ~2% of the strain change at relatively high electric fields (30–35 V/μm) [Fig. 8(B-c)], while those with 30 wt % of the PMMA fractions were largely strained (~16%) at much lower electric fields (20–25 V/μm) [Fig. 8(B-a)]. Surprisingly, these strain changes were almost two times larger than conventional SEBS system (SEBS/oil = 40/60 wt %) even at almost half of the corresponding electric field [Fig. 8(B-d)]. These

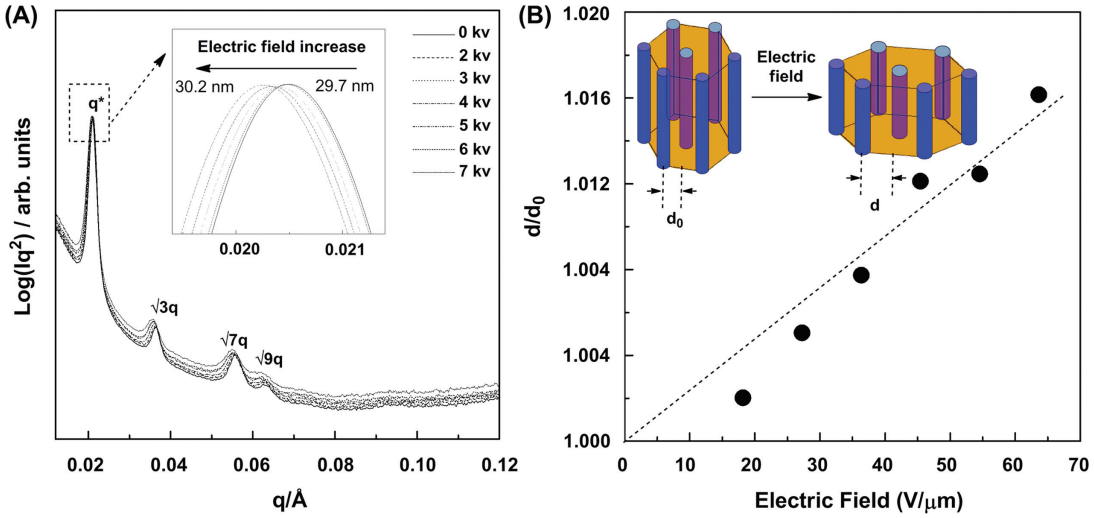

FIGURE 9 Microstructure changes of MMA-DMA-MMA triblock copolymers of 29% of PMMA weight fraction (run 11) by applied voltages. (A) SAXS profiles changes and (B) relative domain size changes.

results showed that softness (Y) and high dielectric constant (k) in DE materials were important factors to increase actuation performance at lower operating voltage because the thickness strain (S_z) changes by maxwell stress were strongly dependent on those two factors. However, the PMDMs with the lower molecular weights [open symbols in Fig. 8(B)] were more easily shorted out in comparison to corresponding higher molecular weight PMDMs [closed symbols in Fig. 8(B)] at relatively lower electric field because of durability problems with smaller molecules.

These strain changes on the actuation performance were further characterized by *in situ* SAXS under electric field to examine their microscopic structure changes, discussed in Figure 5.[19] Figure 9(A) shows SAXS profiles of the PMDM with 29 wt % of the PMMA (run 11) at different applied voltages. Obtained morphology showed well organized hexagonal cylinder structure with 29.7 nm of the domain size ($d = 2\pi/q^*$) with voltage off. This ordered SAXS patterns were gradually shifted to lower scattering vector (q) with increasing the voltage to 7 kV, which indicated that the domain sizes increased by the applied voltages. For example, the domain size was 30.2 nm at 7 kV, which was 0.5 nm larger than that at 0 kV. The relative domain spacing (d/d_0) of the PMDM proportionally increased as the electric field increased [Fig. 9(B)], indicating that the microstructure domains of the PMDM were strongly affected under the applied electric field. From these results, the actuation performances with the PMDMs were strongly dependent on their microstructure as well as polarity (k) and the elasticity (Y), which indicated that the PMDM was one of the best candidates as an electroactive material.

CONCLUSION

Ru-based ATRP system successfully gave well-defined MMA-DMA-MMA triblock copolymers with controlled molecular weights and narrow polydispersities by *in situ* sequential block copolymerization of DMA followed by MMA from a difunctional initiator. Obtained triblock copolymers showed periodically well-organized self-assembled morphologies from BCC to LAM structures both in bulk and in film states depending on the PMMA weight factions. Actuation performance with these triblock copolymers showed relatively large deformations with relatively lower electric fields, especially those with lower PMMA weight fractions, which were strongly relative to their high dielectric constant (k) from the methacrylate groups, elastomeric properties with lower modulus, and well-defined microstructures.

ACKNOWLEDGMENTS

This research was supported by a grant from Korea Institute of Science and Technology (KIST) and partially supported by the industrial strategic technology development program funded by the Ministry of Knowledge Economy, Republic of Korea (10035373). Synchrotron SAXS measurements were performed at the Pohang Light Source (PLS).

REFERENCES AND NOTES

1 P. Brochu, Q. Pei, *Macromol. Rapid. Commun.* **2010,** *31*, 10–36.

2 R. Shankar, T. K. Ghosh, R. J. Spontak, *Soft Matter* **2007,** *3*, 1116–1129.

3 R. Pelrine, R. Kornbluh, Q. Pei, J. Joseph, *Science* **2000,** *287*, 836–839.

4 R. Pelrine, R. Kornbluh, J. Joseph, R. Heydt, Q. Pei, S. Chiba, *Mater. Sci. Eng. C* **2000,** *11*, 89–100.

5 Y. Bar-Cohen, Electroactive Polymer (EAP) Actuators as Arificial Muscles: Reality, Potential, and Challenges, 2nd ed.; SPIE Press, **2004.**

6 L. Bay, K. West, Sommer-P. Larsen, S. Skaarup, M. Benslimane, *Adv. Mater.* **2003,** *15*, 310–313.

7 C. Huang, R. Klein, F. Xia, H. Li, Q. M. Zhang, *Ieee T. Dielect. El. In.* **2004,** *11*, 299–311.

8 R. Shankar, T. K. Ghosh, R. J. Spontak, *Adv. Mater.* **2007,** *19*, 2218–2223.

9 R. E. Pelrine, R. D. Kornbluh, J. P. Joseph, *Sens. Actuators A* **1998,** *64*, 77–85.

10 E. A. Stefanescu, X. Tan, Z. Lin, N. Bowler, M. R. Kessler, *Polymer* **2010,** *51*, 5823–5832.

11 Y. J. Jang, T. Kato, T. Ueki, T. Hirai, *Sens. Actuators A* **2011,** *168*, 300–306.

12 D. P. Chatterjee, B. M. Mandal, *Macromolecules* **2006,** *39*, 9192–9200.

13 S. Coca, K. Matyjaszewski, *J. Polym. Sci. Part A: Polym. Chem.* **1997,** *35*, 3595–3601.

14 J. M. Yu, P. Dubois, R. Jerome, *Macromolecules* **1996,** *29*, 8362–8370.

15 M. Ouchi, T. Terashima, M. Sawamoto, *Chem. Rev.* **2009,** *109*, 4963–5050.

16 W. A. Braunecker, K. Matyjaszewski, *Prog. Polym. Sci.* **2007,** *32*, 93–146.

17 K. Y. Baek, M. Kamigaito, M. Sawamoto, *J. Polym. Sci. Part A: Polym. Chem.* **2002,** *40*, 1937–1944.

18 J. Bolze, J. Kim, J. Huang, S. Rah, H. Youn, *Macromol. Res.* **2002,** *10*, 2–12.

19 B. Kim, Y. D. Park, K. Min, J. H. Lee, S. S. Hwang, S. M. Hong, B. H. Kim, S. O. Kim, C. M. Koo, *Adv. Funct. Mater.* **2011,** *21*, 3242–3249.

20 L. Leibler, *Macromolecules* **1980,** *13*, 1602–1617.

21 I. W. Hamley, The Physics of Block Copolymers, 1st ed.; Oxford Science Publications, **1999.**

22 X. Zhang, B. C. Berry, K. G. Yager, S. Kim, R. L. Jones, S. Satija, D. L. Pickel, J. F. Douglas, A. Karim, *ACS Nano* **2008,** *2*, 2331–2341.

23 S. M. Lai, C. M. Chen, *Eur. Polym. J* **2007,** *43*, 2254–2264.

24 H. L. Kwak, K. Y. Cho, S. G. Yu, K. Y. Baek, J. C. Lee, S. M. Hong, C. M. Koo. *Sens. Actuators A* **2012,** *174*, 547–554.

25 B. Kim, Y. Park, J. Kim, S. M. Hong, C. M. Koo, *J. Polym. Sci. Part A: Polym. Phys.* **2010,** *48*, 2392–2398.